Sensors and Actuators A-Physical, 2008, Vol 147, Iss 2, pp607-612

# Coupled Piezoelectric Fans with Two Degree of Freedom Motion for the Application of Flapping Wing Micro Aerial Vehicles

**Hsien-Chun Chung[1], K. Lal Kummari[1], S. J.Croucher[2], N. J.Lawson[2], S. Guo[2], Z. Huang[1,*]**

[1]Department of Materials, School of Applied Sciences, Cranfield University, Beds, MK43 0AL, UK

[2]Department of Aerospace Engineering, School of Engineering, Cranfield University, Beds, MK43 0AL, UK

[*]Corresponding author e-mail: Z.Huang@Cranfield.ac.uk

## Abstract

Piezoelectric fans consisting of a piezoelectric layer and an elastic metal layer were prepared by epoxy bonding and a coupled flexible wing was formed by a pair of carbon fibre reinforced plastic wing spars and polymer skin attached to two piezoelectric fans. Two sinusoidal voltages with phase differences were then used to drive the coupled piezoelectric fans. High speed digital cameras were used to characterise the two degree of freedom (DOF) motion of the wing and these results were compared to finite element model of the wing and the coupled piezoelectric fans. It has been observed that the phase delay between the driving voltages applied to the coupled piezoelectric fans play an important role in the control of the flapping and twisting motions of the wing and this set-up has the potential for application to the control of flapping wings for micro aerial vehicles.

Keywords: piezoelectric fan, flapping, twisting, resonance, FEM, MAV

## 1 Introduction

The interest in flapping wing micro aerial vehicles (MAV) has resulted in substantial work in recent years [1-3]. A MAV is defined as a semiautonomous airborne vehicle, measuring less than 15 cm in any dimension, weighing no more than 140 grams, which can fly up to 2 hours for a range of 10 km [1]. As demonstrated by flying birds and insects, flapping flight is advantageous for its superior manoeuvrability and lifting capability at low flight speeds [3,4]. Flapping wing systems as inspired by insect flight generally involve the wing completing pitching, yawing and sweeping components of motion over a flapping cycle [5]. Different mechanisms such as pneumatic and motor-driven actuators have been applied to mimic this complex flapping motion, but these mechanisms often suffer from heavy weight and mechanical system complexity [5].

Piezoelectric materials especially lead zircornate titanate (PZT) are widely used in smart structures as sensors and actuators due to their high bandwidth, high output force, compact size, and high power density [6]. However, the piezoelectric effect is intrinsically very small and only a small deflection can be expected directly from the bending piezoelectric unimorph/bimorph. Therefore some kind of motion amplification mechanisms are required to achieve large deflection. Fearing et al. developed piezoelectrically actuated four-bar mechanisms for micromechanical flying insect thorax. [7-9] Cox et al. reported three piezoelectrically activated four bar and five bar linkage systems for the electromechanical emulation of mesoscale flapping flight. [10] Park et al. developed a four bar linkage system driven by lightweight piezo-composite actuator to mimicking the flapping wing system of insects. [11]

A simpler motion amplification mechanism is a piezoelectric fan (piezofan) which couples a piezoelectric unimorph to an attached flexible blade and is capable of producing large deflections especially at resonance. Piezofans were first investigated in the late seventies [12]. In the last a few years the demand for portable electronic devices has brought interest in the use of piezofans as a compact, low power, noiseless air cooling technology for applications such as laptop computers and DVD players etc. [13,14] We have investigated the optimization and characterization of individual piezofan structure at quasi-static and dynamic operations in a separate report [15]. In this paper we report the investigation on using two coupled piezofans in parallel driven by sinusoidal voltages with different phase delays between them to realise the flapping and twisting movements of the wing structure. The main purpose of using piezofan as actuators is to facilitate this simple actuation mechanism to obtain two degree of freedom motion (2DOF), namely the flapping and twisting, of the wing and to develop methods for the control of its 2DOF motion. The experimental and finite element analysis and the effect of phase delay to the flapping and twisting of the wings attached to the coupled piezofans will be presented.

## 2 Experimental

Piezofans were prepared by bonding together a stainless steel metal shim with a piezoelectric PZT patch using epoxy glue EPOTEK 301-2 (Epoxy Technology, US). The PZT wafers (PSI-5H4E) and stainless steel foils (Fe/Cr15/Ni7/Mo2.25) were purchased from commercial sources [15]. The schematic set up for the 2 DOF motion is shown in Fig. 1. The two piezoelectric fans were of the unimorph type, with the PZT patch of the dimensions 30mm x 10mm x 127 μm, and the elastic stainless steel layer of the dimensions 43mm x 10mm x 125 μm, so the total length of the piezoelectric fan was 43 mm. A 3 mm gap existed between the clamping and the start of the PZT patch in order to prevent the ceramic layer from broken during vibration. A pair of spars made of

carbon fibre reinforced plastic (CFRP) connected with a flexible polymer skin formed the wing and the wing was attached to the two piezoelectric fans clamped in parallel to form the coupled fans. The gap between the two fans, therefore also the gap between the two spars, was varied from 10 mm to 2 mm.

The same wave (usually sinusoidal) signal from a function generator was split and supplied to two high voltage amplifiers. One of the split signals was then amplified and applied to one piezofan directly whilst the second signal was connected to an in-house made phase delay circuit (which can achieve 0 to 180 degree phase delay) before being connected to the other amplifier and then the other piezofan. The piezofans were clamped perpendicularly in parallel and both the flapping and twisting motions are in the horizontal direction. This enabled a high speed camera (Photron APX) fixed above the piezofans to record both the flapping the twisting motions of the wing. A frame rate of 2000 frames/s was used with an area of interest of 61.25mm x 61.25mm, which corresponded to a mean resolution of 67 μm per pixel. The camera was controlled by a computer system to record one second of data corresponding to 2000 images. The 2000 images covered several full cycles of the vibration (the frequency was usually between 10 to 100 Hz). The displacement data was then obtained by comparing images over a full cycle and directly analysing the image showing the largest displacement. ANSYS finite element modelling (FEM) was used to model the behaviours of the coupled piezofans and the wing attached to it.

## 3 Results and Discussion

### 3.1 Characterization of the dynamic motions for the coupled piezofans

Fig. 2 shows the results of the FEM modal analysis. The first mode was pure bending or flapping, at 23.7 Hz (a). The second mode was pure twisting (b), at 58 Hz and the third mode contained both bending and twisting at 62.9 Hz. The material parameters used in the FEM are listed in Table I.

Figure 3 shows typical pictures produced by superimposing two high speed camera images of the two extreme positions of the wing within a vibration cycle, without any phase delay between the two input voltages 170 $V_{pp}$ at frequencies (a) 22.3 and (b) 47.4 Hz. Both the flapping and twisting motion of the wing were obtained. It was found that the flapping displacement was peaked at 20 mm at the frequency 22.3.Hz. The twisting motion was found peaked at 16º at the frequency 47.4 Hz. Figure 4 shows the flapping and twisting amplitudes as functions of frequency for the wing. The quantitative discrepancy on the mode frequencies between the FEM modelled and actually measured values could be contributed to a number of factors. These include the uncertainty of the Young's modulus for the CFRB spars and the polymer skin used in the FEA modelling, the non-perfect clamping at the foot of the piezofans, and probably most importantly the unmatched piezofans to drive the wing. A number of these factors will now be discussed in more detail.

(1) Unmatched piezofans: for the system shown in figure 1, if piezofan I and II were identical, with no phase difference between the two input signals (i.e. phase delay = 0), the two piezofans would be expected to vibrate in parallel at around the first resonant frequency. However, for many reasons it is not possible to have two identical piezofans in terms of their resonant frequencies and vibration amplitudes. As every piezofan is produced individually, any difference in the width and length of the PZT patch and the stainless steel shim, the relative position of the PZT patch on the metal shim, and the exact clamping conditions etc, all can lead to the variation of the resonant frequency and amplitude. Furthermore, the vibration amplitude also depends on the exact piezoelectric coefficient of the PZT patch and the condition of the bonding layer, as well as the

geometrical factors. This means that, at any frequency, even at phase delay=0, the two piezofans may not vibrate in parallel, or one may vibrate with a larger amplitude than the other. This will show an apparent twisting motion for the wing. Since, around the first resonant frequency, the flapping displacement is at a maximum this mismatch in piezofan displacement appears to be at its greatest. For this reason, the spread of the measurement data of the twisting motion around the first resonant frequencies is expected to be the largest, as confirmed by measurements (Figure 4). The effect of different resonant frequency on the flapping motion of the wing was found to be much smaller, as shown in Figure 4, where the flapping motion around the second resonance was smaller relative to the flapping motion at the first resonant frequency.

(2) Stiffness of the wing skin materials: the flapping and the twisting motions of the wing also depend very much on the stiffness of the wing skin material, as well as the piezofan actuators. We consider two extreme cases here: (i) If the skin material is infinitely soft (the stiffness coefficient $c_{ij}$=0), the whole system as shown in Figure 1 will act like two independent piezofans. At any frequency, the two piezofans will vibrate in parallel when the phase-delay = 0 and in anti-phase when the phase-delay = 180 º. The flapping amplitude will be at its maximum when the phase-delay = 0 and reduce to zero when the phase-delay = 180 º, and the twisting motion will be at its maximum when the phase-delay = 180º and reduce to zero when the phase-delay = 0. Changing the phase-delay will change the flapping and twisting amplitudes of the wing. However, if there is a difference of the 1$^{st}$ resonant frequencies $f_1$ and $f_2$ of the two piezofans, the flapping and apparent twisting will depend on the operating frequency f and the value of $f_2$- $f_1$. (ii) If the skin material is infinitely stiff (the compliance coefficients $s_{ij}$=0), then the whole system must be treated as a single body and it has its unique resonant frequencies, the first mode being bending and the second mode being twisting. In this case, the resonant frequency of the individual actuator piezofan I and II or the difference between the two will have a limited effect on the performance of the wing. In fact, the actual wing

will be between the above two extremes, with a finite stiffness coefficients $c_{ij}>0$. The system has its unique bending and twisting mode resonance frequencies but the performance could be affected by the difference in resonant frequencies of the individual piezofan actuators. Every effort was made to fabricate the piezofans as identical as possible. The effect of different skin materials is a subject for further study. It is expected that a thin and light but stiff material--like an insect wing, is the best.

3.2 Two DOF motion control by phase differentiated drive

Figure 5 illustrates measurement results of (a) the flapping and (b) twisting vibration amplitudes of the wing as functions of operating frequency under two input voltages 170 $V_{pp}$ with different phase delays between them. The gap between the two piezofans was 10 cm. It can be observed that the flapping motion had a resonance at around 22 Hz, and the vibration amplitude was the largest at phase-delay = 0 and reduced with the increasing phase-delay. The amplitude reached a minimum when the phase-delay equalled 180°, about a quarter of the value at the phase-delay = 0. The twisting motion peaked around 49 Hz, and, contrary to the flapping, its amplitude increased with the increasing phase-delay. The twisting amplitude for the phase-delay = 0 was about half of the value for the phase-delay = 180°. However, as discussed in the last section, the amplitude mismatch generated twisting movement was significant for the frequencies near the flapping resonance, when there was inevitably a difference of the resonant frequency between the two piezofans. The slight increase of the flapping motion around the frequency 50 Hz may also due to the increase of the amplitude mismatch around the twisting resonance there.

Figures 5 shows that it is possible to change both the flapping and twisting motions of the flapping wing simply by varying the phase-delay between the two input signals. At frequencies around the 1st resonance, i.e. the flapping mode resonance, increasing the phase-delay from 0 to 180° lead to the reduced flapping motion. At frequencies around the 2nd resonance, i.e. the twisting mode resonance,

increasing the phase-delay from 0 to 180º lead to increased twisting motion. However, due to the difficulty in obtaining matched piezofan actuators, it is not clear from this study what are the effects of changing phase-delay on the twisting motion around the flapping resonant frequency, and the effects on the flapping motion around the twisting resonant frequency. Nevertheless, the flapping at frequencies far away from the flapping resonance was found to be insignificant.

**3.3** The effect of the gap distance between the two piezofans

The effect of the distance between the two piezofan actuators on the flapping and twisting motions of the wing was also investigated. Both the flapping and twisting were recorded at their respective resonant frequencies. For example, the flapping were measured at 26.2, 26.3, 26.0 and 26.2 Hz for gap distances 10, 8, 5 and 2 mm, respectively; and the twist angles were measured at 53.6, 49.1, 51.4 and 47.4 Hz for gap distances 10, 8, 5 and 2 mm, respectively. Changing the gap distance involves de-clamping at least one of the piezofan, varying the distance between the two piezofans, and then re-clamping the piezofans. These results show that the flapping resonant frequency of the system changed a small amount (e.g. from 26.0 to 26.3 Hz) after these manoeuvres, but noticeable difference in twisting resonant frequencies (from 47.4 to 53.6 Hz) resulted. However, these changes were not monotonic with the change of the gap distance and were therefore most likely to be due to the change of the effective clamping distances in the re-clamping, which leads to the change of the resonant frequency of the piezofan, as discussed before.

Figure 6 shows the measured phase delay dependence of (a) the bending displacement and (b) the twisting angle for the same system. The measured values were represented by symbols ♦, □, ▲, and x and their corresponding polynomial fittings by solid, dashed, dotted, dash and dotted curves for the gap equals to 10, 8, 5 and 2 mm respectively. The effect of the gap distance between the two fans was also investigated and results were also shown in the figure. When the gap distance was 10 mm and the voltages $V_{pp}$=170 V applied to the two piezoelectric fans were in phase (phase delay = 0º), the amplitude of the bending movement of the wing reached 23.4 mm and resonated at 26.2 Hz. If the phase delay of the two driving voltages was increased and all the other conditions remained the same, the mode of the wing movement remained the pure bending and also resonated at the same frequency, but with a reduced amplitude. In addition, if the two driving voltages were anti-

parallel (phase delay = 180º), the amplitude of the resonant bending displacement was reduced to minimum of 1.8 mm. When the gap between the two wing spars was reduced from 10 mm to 8 mm (and further to 5 and 2 mm) and all the other conditions were kept the same, the bending displacement increased but the dependence on the phase delay was similar (Fig. 6a).

If the frequency of the two driving voltages was increased from 26.2 Hz to 53.6 Hz, the same as its second mode frequency, the wing motion became a pure twisting. In this case, the two wing spars as represented by point 1 and point 2 in Fig. 1 were always moving in the opposite directions with the middle line not moving. When the gap distance was 10 mm and the voltages $V_{pp}$=170 V applied to the two piezofans were in phase (phase delay = 0º), the twisting angle of the wing was minute, close to 0 degree at 53.6 Hz. If the phase delay of the two driving voltage was increased and all the other conditions remained the same, the wing movement was found to remain at the pure twisting mode and also resonate at the same frequency, but with an increased twisting amplitude. For the case with the two driving voltages set to anti-parallel (phase delay = 180º), the resonant twisting angle reached 41º (Fig. 6b). It was also found, if the gap between the two wing spars was reduced from 10 mm to 8 mm (and further to 5 and 2 mm) and all the other conditions were kept the same, the wing twisting increased but its dependence on the phase delay was similar (Fig. 6b).

The motional amplitude dependence on the gap distance between the two spars could be interpreted by consideration of the air damping effect. In this case, the damping of the wing movement would increase in proportion to its cross sectional area where the effective cross section of the wing is proportional to the gap distance [16]. So the reduced gap distance would lead to a reduced aerodynamic damping and hence an increased vibration amplitude. To this end, a nearly linear relationship (with negative slump rates) was found to exist between both the bending and twisting amplitudes and the gap distance (Fig. 7), further reinforcing this proposed damping dependency.

## 4 Conclusions

Coupled piezoelectric fans were formed by clamping two fans in parallel and attaching a flexible wing made of two stiff carbon fibre reinforced plastic wing spars and a soft polymer skin. The dynamic behaviours of the wing were modelled by FEM modal analysis and investigated by using high speed digital cameras. It was found both the mode and the amplitude of the wing motion depend strongly on frequency. The degrees of motion of the wing increased by nearly 10 times at resonant frequencies as compared to the motion at frequencies far away from the resonance. It was found that the phase delay between the driving voltages supplied to the two coupled piezoelectric fans play a critical role in the control of the flapping and twisting motions of the wing. The bending amplitude of the wing reduced with the increasing phase delay and the twisting movement increased with an increasing phase delay.

**Acknowledgements**

This work was financially supported by the UK EPSRC Grant Flapping Wing MAV EP/C511190/1 and Platform Grant EP/D506638/1. We thank Prof. R. W. Whatmore of Tyndall National Institute, Ireland for invaluable discussions.

## References


[1] W. Shyy, M. Berg and D. Ljungqvist, Flapping and flexible wings for biological and micro air vehicles, Prog. in Aerospace Sci. 35 (1999) 455-505.

[2] D. L. Raney and E. C. Slominski, Mechanization and control concepts for biologically inspired micro aerial vehicles, AIAA 2003-5354, AIAA Guidance, Navigation and Control Conference, Austin, Texas, Aug. 2003.

[3] C.P. Ellington, The novel aerodynamics of insect flight:applications to micro-air vehicles, Journal of Experimental Biology 202 (1999) 3439-3448.

[4] C.P. Ellington, C. van den Berg, A.P. Willmott, and A. Thomas, Leading-edge vortices in insect flight, Nature 384 (1996) 626-630.

[5] M. H. Dickinson, F. Lehmann, and S. Sane, Wing rotation and the aerodynamic basis of insect flight, Science 284 (1999) 1954-1960.

[6] C. Niezrecki, D. Brei, S. Balakrishnan, and A. Moskalik, Piezoelectric actuation: state of the art, The shock and vibration digest. 33 (2001) 269-280.

[7] R.S. Fearing, K.H. Chiang, M.H. Dickinson, D.L. Pick, M. Sitti, and J. Yan, Wing transmission for a micromechanical flying insect, in: Proc. IEEE Int. Conf. Robotics and Automation, San Francisco, CA, USA, 2000, pp. 1509-1516.

[8] M. Sitti, PZT actuated four bar mechanism with two flexible links for micromechanical flying insect thorax, in: IEEE Int. Conf. Robotics and Automation, South Korea, 2001, pp.3893-3900.

[9] J. Yan, R.J. Wood, S. Avadhanula, M. Sitti, and R.S. Fearing,Towards flapping wing control for a micromechanical flying insect, in: IEEE Int. Conf. Robotics and Automation, South Korea, 2001, pp.3901-3908.

[10] A. Cox, D. Monopoli, D. Cveticanin, M. Goldfarb, and E. Garcia, The development of elastodynamic components for piezoelectrically actuated flapping micro air vehicles, J. Intelli. Mat. Syst. and Struct. 13 (2002) 611-615.

[11] H.C. Park, K. J. Kim, S. Lee, S. Y. Lee, Y. J. Cha, K. J. Yoon, and N. S. Goo, Biomimetic Flapping Devices Powered by Artificial Muscle Actuators, in: UKC2004 US-Korea Conference on Science, Technology and Entrepreneurship, August, 2004.

[12] M. Toda, Voltage-induced large amplitude bending device-PVF2 bimorph-its properties and applications, Ferroelectrics. 32 (1981) 911.

[13] J. Yoo, J. Hong, and W. Cao, Piezoelectric ceramic bimorph coupled to thin metal plate as cooling fan for electronic devices, Sensors &Actuators A 79 (2000) 8-12.

[14] T. Wu, P. Ro, A. Kingon, and J. Mulling, Piezoelectric resonating structures for microelectronic cooling, Smart. Mater. Struct. 12 (2003) 181-187.

[15] Hsien-Chun Chung, K. Lal Kummari, S. J.Croucher, N. J.Lawson, E. Liani, S. Guo, and Z. Huang, Development of Piezoelectric fans for loaded applications, submitted to Sensors and Actuators A.

[16] Joseph Katz and Allen Plotkin, Low-Speed Aerodynamics, Cambridge University Press, 2nd edition, 2005.

Figure Captions

Fig. 1 The schematic set up for the coupled piezoelectric fans with the attached wing and their vibration measurement by high speed camera photography.

Fig. 2 The finite element modelling modal analysis for the coupled piezoelectric fans systems as shown in figure 1: (a) $1^{st}$ mode bending -23.7 Hz; (b) $2^{nd}$ mode twisting -58 Hz.

Fig. 3 Typical images produced by superimposing two high speed camera images of the two extreme positions of the wing within a vibration cycle at frequencies (a) 22.3 and (b) 47.4 Hz. The driving voltage was 170 $V_{pp}$.

Fig. 4 The measured flapping and twisting motion amplitudes of the wing as functions of the operating frequency driving by the two coupled piezofans under 170 $V_{pp}$.

Fig. 5 The measured vibration amplitudes as functions of frequency at different phase-delays at around (a) the flapping and (b) the twisting resonances.

Fig. 6 The phase delay dependence of the vibration amplitude of the bending and twisting modes of the wing driving by the coupled piezoelectric fans under 170 $V_{pp}$ at different gap distances between the two spars: (a) bending mode; (b) twisting mode.

Fig. 7 The vibration amplitudes of the bending and twisting motions of the wing as functions of the gap distance between the two spars. The nearly linear relationships suggests that the air damping effect was responsible for the decreasing vibration amplitude with the increasing gap distance.

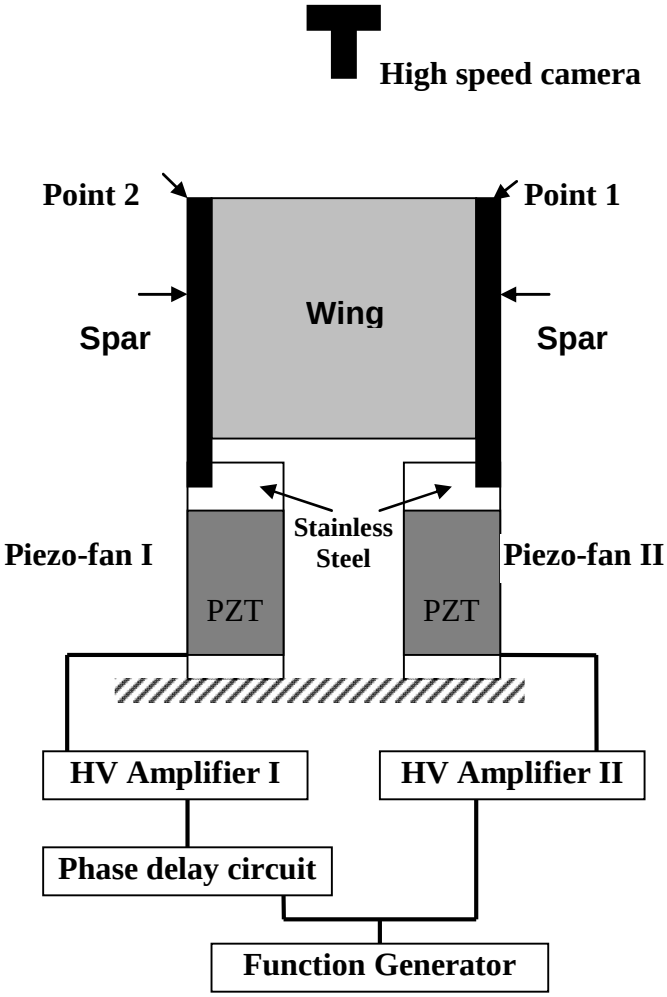
High speed camera
Point 2
Point 1
Wing
Spar
Spar
Stainless Steel
Piezo-fan I
Piezo-fan II
PZT
PZT
HV Amplifier I
HV Amplifier II
Phase delay circuit
Function Generator

Fig. 1

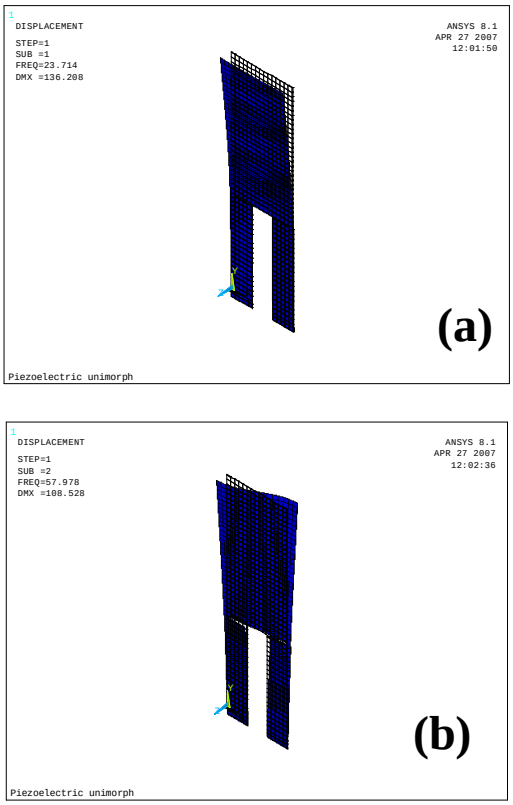
1
DISPLACEMENT
STEP=1
SUB =1
FREQ=23.714
DMX =136.208
ANSYS 8.1
APR 27 2007
12:01:50
(a)
Piezoelectric unimorph
1
DISPLACEMENT
STEP=1
SUB =2
FREQ=57.978
DMX =108.528
ANSYS 8.1
APR 27 2007
12:02:36
(b)
Piezoelectric unimorph

Fig. 2

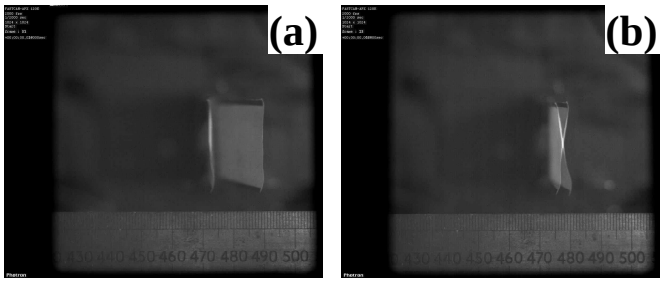


Fig. 3

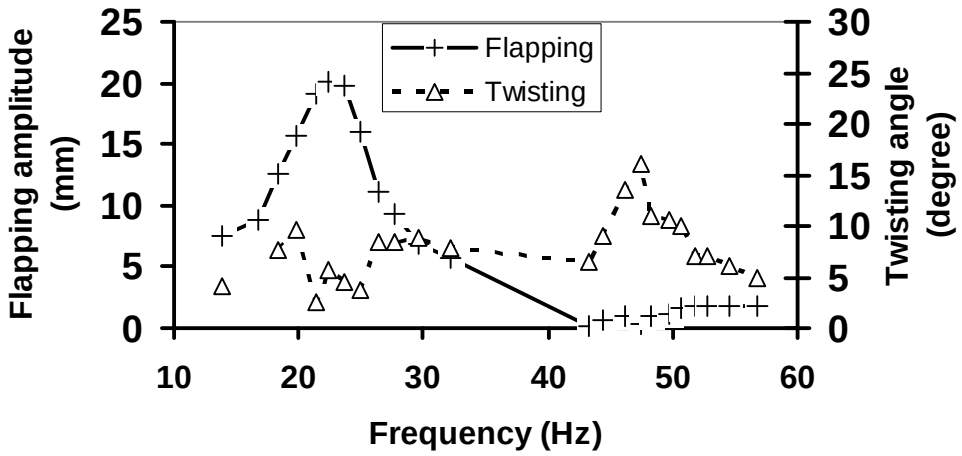
Flapping amplitude (mm)
Twisting angle (degree)
Flapping
Twisting
Frequency (Hz)
0
5
10
15
20
25
30
10
20
30
40
50
60

Fig. 4

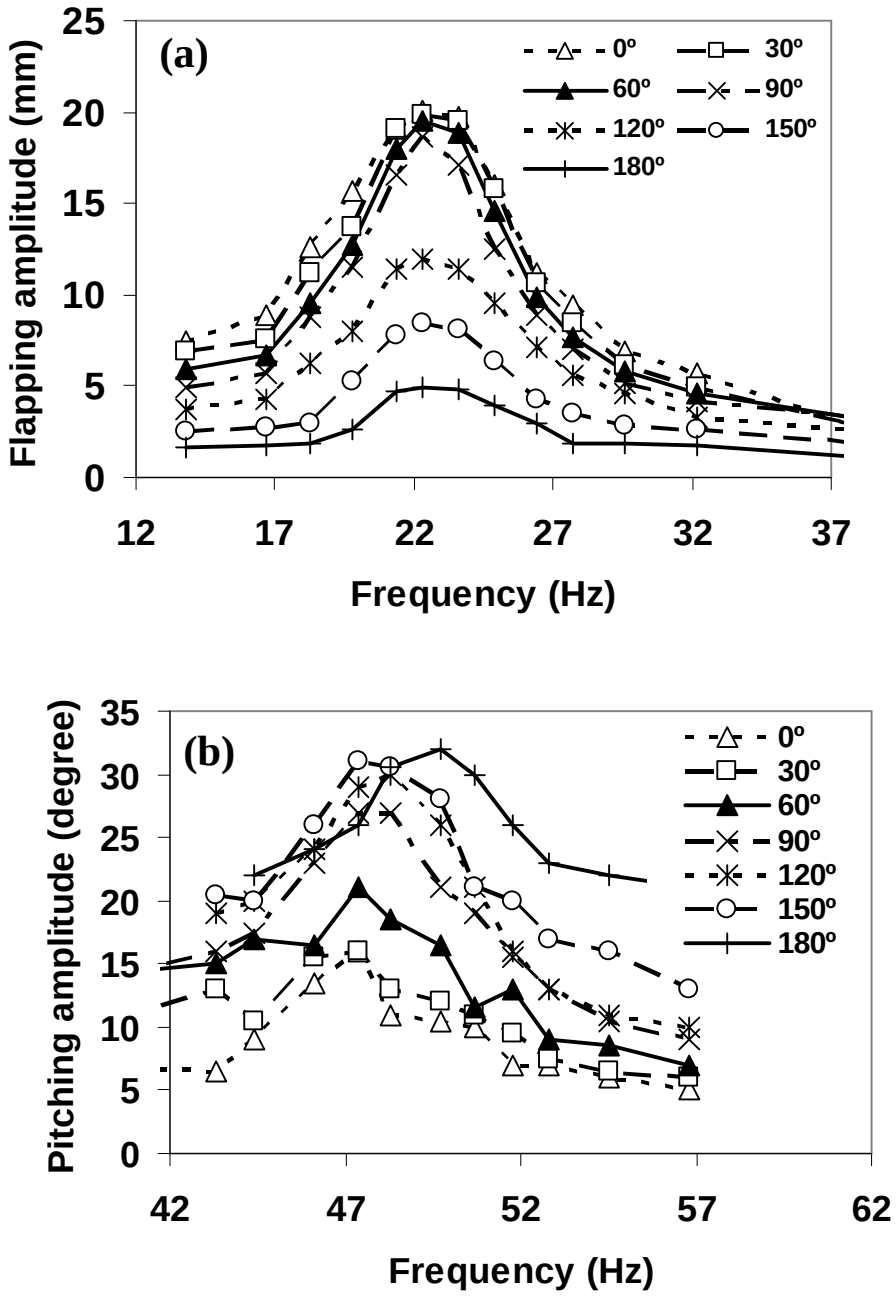
(a)
0º
30º
60º
90º
120º
150º
180º
Flapping amplitude (mm)
0
5
10
15
20
25
12
17
22
27
32
37
Frequency (Hz)
(b)
0º
30º
60º
90º
120º
150º
180º
Pitching amplitude (degree)
0
5
10
15
20
25
30
35
42
47
52
57
62
Frequency (Hz)

Fig. 5

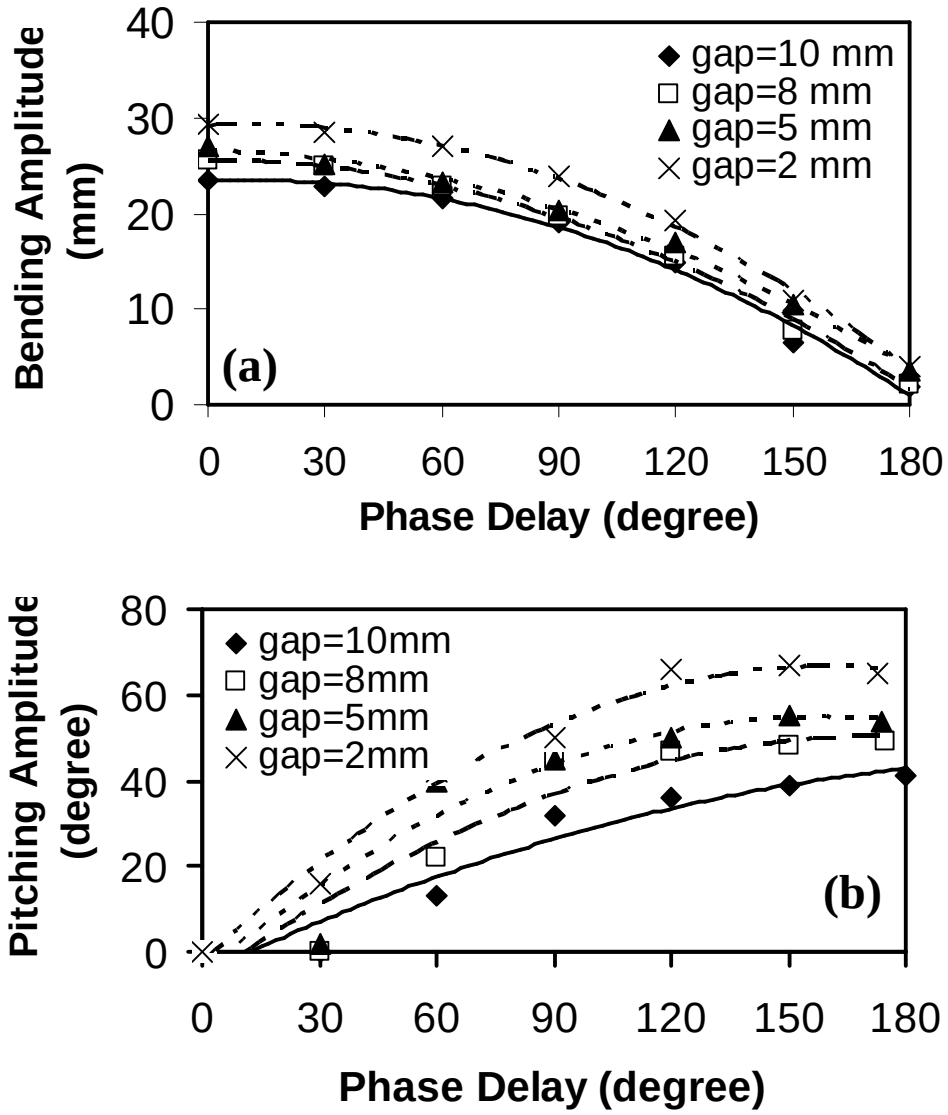
Bending Amplitude (mm)
40
30
20
10
0
gap=10 mm
gap=8 mm
gap=5 mm
gap=2 mm
(a)
0
30
60
90
120
150
180
Phase Delay (degree)
Pitching Amplitude (degree)
80
60
40
20
0
gap=10mm
gap=8mm
gap=5mm
gap=2mm
(b)
0
30
60
90
120
150
180
Phase Delay (degree)

Fig. 6

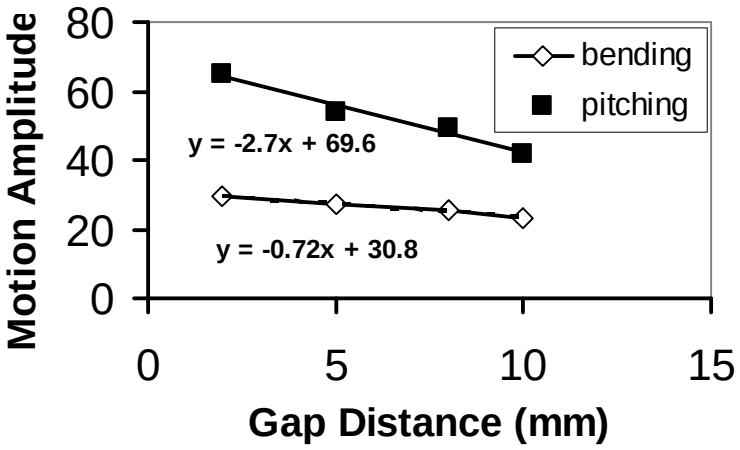
Motion Amplitude
80
60
40
20
0
0
5
10
15
Gap Distance (mm)
bending
pitching
y = -2.7x + 69.6
y = -0.72x + 30.8

Fig. 7

Table I: Material property parameters used for the finite element modelling.

| **Material** | **PZT 5H** | **Stainless Steel** | **Polymer** | **CFRB** |
|---|---|---|---|---|
| Thickness (μm) | 127 | 125 | 50 | 100 |
| Width (mm) | 10 | 10 | - | 2 |
| Young's Modulus (GPa) | 62 | 200 | 8 | 200 |
| Density (Kg/ $m^3$) | 7800 | 7900 | 1534 | 1750 |
| Poisson's ratio | — | 0.28 | 0.27 | 0.27 |
| $d_{31}(10^{-12}$ m/V) | -320 | — | — | — |
| $\varepsilon_{11}$ | 3130 | — | — | — |
| $\varepsilon_{22}$ | 3130 | — | — | — |
| $\varepsilon_{33}$ | 3400 | — | — | — |
| $e_{31}$ | -12 | — | — | — |
| $e_{33}$ | 22.22 | — | — | — |
| $e_{15}$ | 19.39 | — | — | — |
| $c_{11}(10^9$ N/$m^2$) | 126 | 255.68 | — | — |
| $c_{12}(10^9$ N/$m^2$) | 79.5 | 99.43 | — | — |
| $c_{13}(10^9$ N/$m^2$) | 84.1 | — | — | — |
| $c_{33}(10^9$ N/$m^2$) | 117 | — | — | — |
| $c_{44}(10^9$ N/$m^2$) | 23.0 | 78.13 | — | — |